The depth of the shower maximum of air showers measured with AERA

Bjarni Pont[a,*] **for the Pierre Auger Collaboration**[b,†]

[a]*Department of Astrophysics/IMAPP, Radboud University, P.O. Box 9010, NL-6500 GL Nijmegen, The Netherlands*

[b]*Observatorio Pierre Auger, Av. San Martín Norte 304, 5613 Malargüe, Argentina*

E-mail: b.pont@science.ru.nl, spokespersons@auger.org

The Auger Engineering Radio Array (AERA) is an array of 153 radio antennas spanning an area of $17\,\mathrm{km}^2$, currently the largest of its kind, that probes the nature of ultra-high energy cosmic rays at energies around the transition from Galactic to extra-galactic origin. It measures the MHz radio emission of extensive air showers produced by cosmic rays hitting our atmosphere. The elemental composition of cosmic rays is a crucial piece of information in determining what the sources of cosmic rays are and how cosmic rays are accelerated. This composition can be obtained from the mass-sensitive parameter $X_{\max}$, the depth of the shower maximum. We reconstruct $X_{\max}$ with a likelihood analysis by comparing the measured radio footprint on the ground to an ensemble of footprints from Monte-Carlo CORSIKA/CoREAS air shower simulations. We compare our $X_{\max}$ reconstruction with fluorescence $X_{\max}$ measurements on a per-event basis, a setup unique to the Pierre Auger Observatory, and show the methods to be compatible. Furthermore, we extensively validate our reconstruction by identifying and correcting for systematic uncertainties. We determine the resolution of our method as a function of energy and reach a precision better than $15\,\mathrm{g\,cm}^{-2}$ at the highest energies. With a bias-free set of around 600 showers, we find a light to light-mixed composition at energies between $10^{17.5}$ to $10^{18.8}$ eV, also in agreement with Auger fluorescence measurements.

*Speaker

†Full author list at https://www.auger.org/archive/authors_2022_06.html

PoS(ARENA2022)044

1. AERA and using X_{max} for Mass Composition Studies

The *Auger Engineering Radio Array* (AERA) [1] is an array of 153 radio antenna stations, spanning an area of about $17\,km^2$. It is part of the Pierre Auger Observatory, located in Argentina. AERA has been built up in stages, using multiple antenna types (primarily LPDA and Butterfly antennas) at various spacings, ranging from 144 to 750 m. Each station consists of two dipole antennas. The array has been designed to measure the radio emission of extensive air showers in the frequency range of 30 to 80 MHz. It is sensitive to the energy range of roughly 10^{17} to 10^{19} eV.

The radio signal footprint measured with multiple antennas encodes the information of the development of the extensive air shower. It thus contains information about the primary cosmic ray that induced the shower. The depth in the atmosphere where the shower is maximally developed, X_{max}, can provide information about the primary cosmic-ray particle. The radio measurements are sensitive to X_{max} because the shape of the radio footprint on the ground depends on where in the atmosphere the air shower developed. Generally, heavier particles interact higher up in the atmosphere because they essentially behave as a superposition of lower-energy protons. This leads to wider footprints of radio emission on the ground than for lighter particles. Because of shower-to-shower fluctuations, the distribution of X_{max} approximately follows a Gumbel distribution [2]; the exact shape of which depends on the mass of the cosmic-ray primaries. From the X_{max} distribution of many measured showers, one can thus make inferences about the overall mass composition.

Here were discuss a method to reconstruct X_{max} for air showers measured at AERA, the resolution that can be achieved, direct comparisons to fluorescence measurements of X_{max}, and the moments of the distribution of X_{max} as obtained by AERA.

2. Event Selection and Reconstruction

We have analysed 7 years of data between 2013 and 2019 and have obtained 2153 high-quality air showers at zenith angles below 55 degrees. Each of these showers has been triggered by the *surface detector* (SD) and thus also provides us with a measurement of the shower energy. To guarantee the quality of the shower measurements various quality cuts were applied. An automated monitoring tool has been implemented that periodically measures the radio background at each station. It detects and rejects periods of excessive RFI and station malfunction that could negatively affect the shower reconstruction. Next, we cut events measured in enhanced atmospheric electric field conditions, such as occur during thunderstorms. For the reconstruction of X_{max} we also require at least 5 radio stations with a good signal. For this, we require a *signal-to-noise ratio* (SNR) of at least 10 (SNR is defined as the square of the maximum amplitude of the radio trace in the signal window, divided by the square of the RMS of the radio trace away from the signal window). Finally, we reject any mis-reconstructions and we require the radio and SD shower core positions to match within 400 m and their shower zenith and azimuth angles within 10°. For a subset of the 2153 showers that pass these criteria, there is also a good FD reconstruction available. For a total of 53 showers, we have both a good radio and FD measurement of X_{max} available. This provides us with a powerful tool to perform an event-to-event comparison of X_{max} of the two methods.
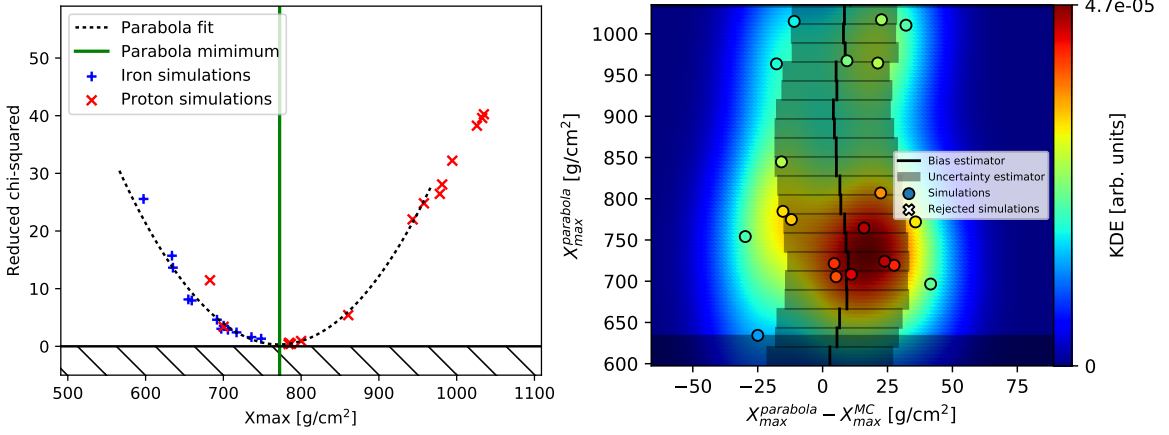
Figure 1: (Left) Parabola fit to the reduced chi-square between the energy fluences of a single measured shower and the ensemble of the simulated proton (red) and iron showers (blue). The minimum (green line) provides an estimation of the $X_{\max}$ of the measured shower. The hatched region masks the unphysical negative region for visibility. (Right) Reconstructed parabola $X_{\max}$ values determined for each of the simulations in the ensemble versus the deviation to their true simulated values (points). A KDE model (colored background) is created to obtain an estimation of the bias in the parabola $X_{\max}$ estimation (center of black bars) and the uncertainty in the $X_{\max}$ reconstruction (width of the black bars). Values not compatible with the bias and uncertainty estimation are rejected and this part of the KDE model is flagged to guarantee that an $X_{\max}$ reconstruction is only accepted if there is a valid bias and uncertainty estimate (no rejections in this example). Similarly, the shaded region indicates flagging where the model would go too far beyond the extent of the underlying data. Further details on these quality checks are available in [9]).

3. Reconstruction of $X_{\max}$

To extract the $X_{\max}$ information from the radio footprint we use a simulation-fitting method, building upon [3]. For each of the measured showers, we create an ensemble of CORSIKA (v7.7100) [4] air shower simulations, with the radio extension CoREAS [5], high-energy interaction model QGSJetII-04 [6], low-energy interaction model UrQMD 1.3cr [7], and the *Global Data Assimilation System* (GDAS)[8] to get the atmospheric model at the time and location of our air showers. The ensemble of simulations consists of 15 proton showers and 12 iron nuclei showers, where the height of the first interaction has been chosen such that the range of possible $X_{\max}$ values is fully covered (as predicted by simulations). Each of these simulated showers is reconstructed in the same way as the measured showers (i.e., the same reconstruction pipeline), allowing for direct comparison. The comparison is done by minimizing the difference in the energy fluences of the stations of the measured shower and the set of simulated showers. We define the chi-square measure between a simulation and the measured shower as:

$$\chi^2 = \sum_{\text{stations}} \frac{(u_{\text{measured}} - S \cdot u_{\text{simulated}}(\vec{r}_{\text{shift}}))^2}{\sigma^2_{u_{\text{measured}}}}, \tag{1}$$

where u is the energy fluence and σ the uncertainty on the energy fluence, and S and $\vec{r}_{\text{shift}}$ free parameters. The shower core location of the simulated showers comes from the radio-reconstructed core of the measured shower and thus has some uncertainty. Hence we allow a core shift $\vec{r}_{\text{shift}}$ as a free parameter in the global minimization. The energy of the simulated shower comes from
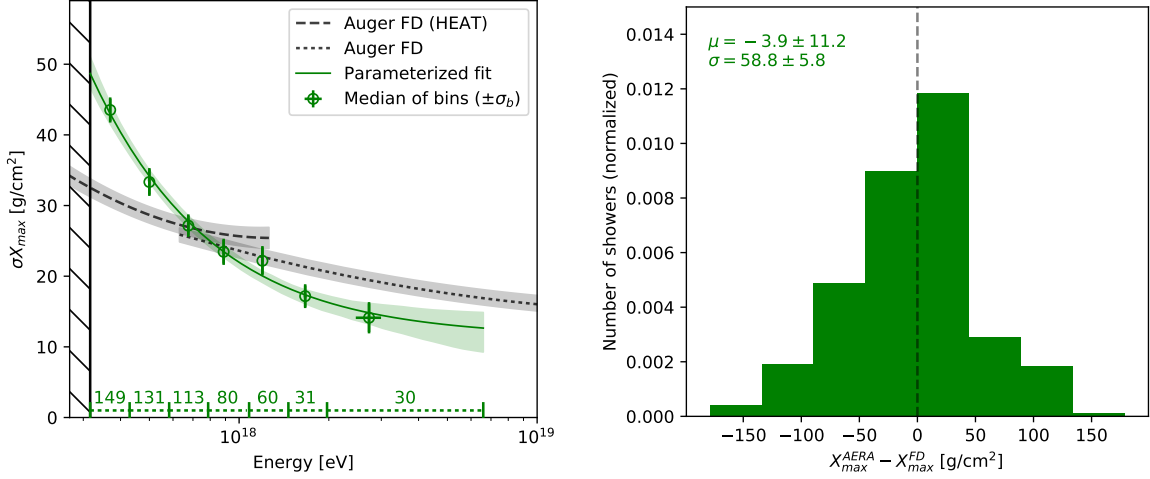
Figure 2: (Left) Median resolution of $X_{\max}$ as a function of shower energy, shown in 7 energy bins (points, shown with bootstrapped uncertainties) and with fitted function (green line). For comparison resolutions of the Auger FD are shown (black lines). The inset at the bottom shows the extent of the energy bins and the number of showers in each bin. (Right) Comparison of $X_{\max}$ for 53 showers independently obtained from radio and fluorescence measurements. Shown at the top are the mean offset and the spread of the data points [$\mathrm{g\,cm^{-2}}$], calculated with bootstrap resampling.

the SD energy estimation and also has an uncertainty, so also a scaling in the energy fluence S is introduced. Values for the free parameters are obtained by minimizing chi-square for each of the 27 simulations simultaneously. This is done in an iterative procedure where the parameter space of the free parameters is stepped through with a gradient descent algorithm (SciPy *basinhopping*). At each step, chi-square is calculated for all simulations and a parabola is fitted to the chi-square values as a function of $X_{\max}$ of the simulations. Fig. 1 (left) shows an example of this for the last iteration step. At each step also the quality of the parabola was checked (see [9] for more details). Once the minimization finds a global optimum we can use the minimum of the final parabola as an estimation of $X_{\max}$ of the measured shower.

This is not guaranteed to be a bias-free estimator of $X_{\max}$ because the stability of the parabola function and how much it is constrained varies depending on whether the minimum lies near the edges of the simulated $X_{\max}$ range or near the center. This is, in particular, important for sparse radio arrays, such as AERA, where typically only a handful of stations are available to constrain our minimization. Hence, we introduce a procedure where we determine the reconstruction bias and uncertainty for each event. For this, we reconstruct each of the 27 simulated showers for that event in the same way as we would reconstruct the measured shower (including adding measured radio background signals to the pure simulated signals). Fig. 1 (right) shows an example of the reconstructed $X_{\max}$ from the parabola minimum versus simulated (MC) $X_{\max}$. A two-dimensional *kernel density estimator* (KDE) is applied to the 27 points to parameterize the bias (deviation from the MC values as a function of $X_{\max}^{\mathrm{parabola}}$) and 1σ uncertainty (the spread around the bias). This is then used to correct the parabola $X_{\max}$ from the measured shower and to determine the uncertainty of this $X_{\max}$ estimation. This procedure is performed for each measured shower individually to obtain the bias-corrected $X_{\max}$, from now on called just $X_{\max}$, and its uncertainty $\sigma X_{\max}$.
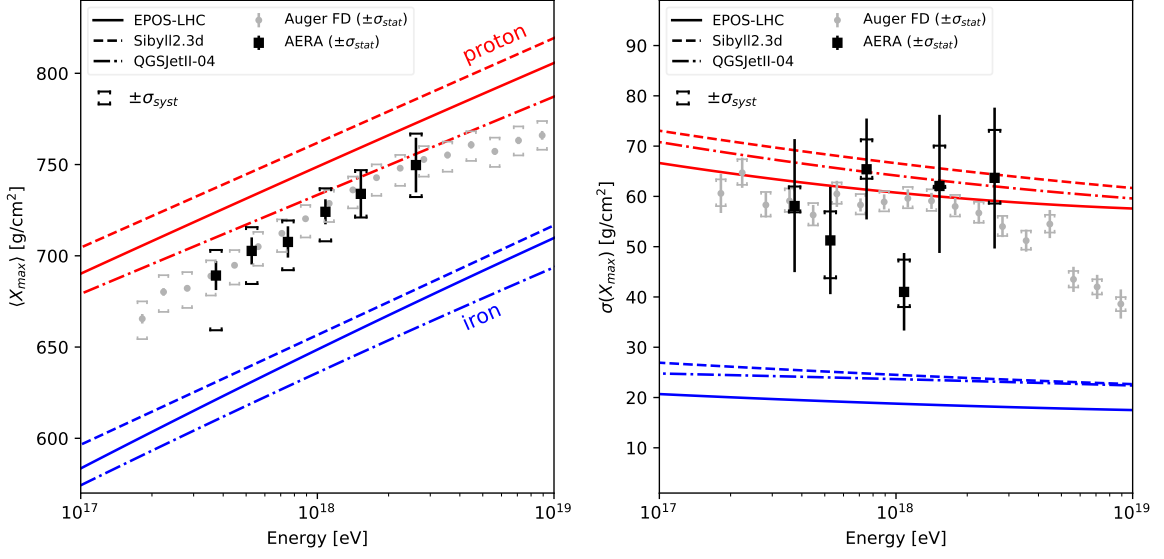
Figure 3: Mean (left) and width (right) of the $X_{\max}$ distribution as measured by AERA in this work (black). The results are compared to predictions from CORSIKA air shower simulations for three hadronic interaction models (lines) for proton (red) and iron (blue) mass compositions [11]. Results from the Auger FD [11] (gray) are shown for comparison.

4. Resolution in $X_{\max}$

In Fig. 2 (left) we show the median resolution as a function of shower energy that we obtain with our method (green points). We fit this with a function, inspired by the resolution in the energy of electromagnetic calorimeters [10]:

$$\sigma X_{\max} = a \cdot \sqrt{\frac{10^{18}\text{eV}}{E}} \oplus b \cdot \frac{10^{18}\text{eV}}{E} \oplus c, \qquad (2)$$

where $a = 13.8 \pm 6.5\,\text{g cm}^{-2}$, $b = 12.8 \pm 2.1\,\text{g cm}^{-2}$, and $c = 11.3 \pm 4.5\,\text{g cm}^{-2}$ and $\oplus$ indicates the quadratic sum. With this, we show a resolution of better than $15\,\text{g cm}^{-2}$ can be obtained with our method for AERA, a rather sparse radio array. At lower energies, the resolution decreases, mainly driven by the radio SNR decreasing rapidly at lower energies. Furthermore, Fig. 2 also shows the radio technique to be competitive with the Auger fluorescence measurements [11] at the same energies.

5. Comparison of Radio-Fluorescence Hybrid Showers

For 53 events we have independent $X_{\max}$ measurements from both AERA and the Auger FD [12]. Fig. 2 (right) shows the difference of $X_{\max}$ in a (weighted) histogram. We show that there is no significant bias between fluorescence and radio methods for $X_{\max}$ reconstruction ($-3.9 \pm 11.2\,\text{g cm}^{-2}$). This is of particular importance because this comparison is independent of selection effects (unlike comparisons of $X_{\max}$ distributions). The compatibility provides an independent check on the validity of fluorescence measurements and furthermore provides us with new constraints on shower physics. In particular, considering that the hadronic part of the shower is arguably less

well understood, as shown by a measured muon deficit w.r.t. simulations, the constraints on the $X_{\max}$ scale between FD and radio provide a new hint in solving the muon puzzle [13].

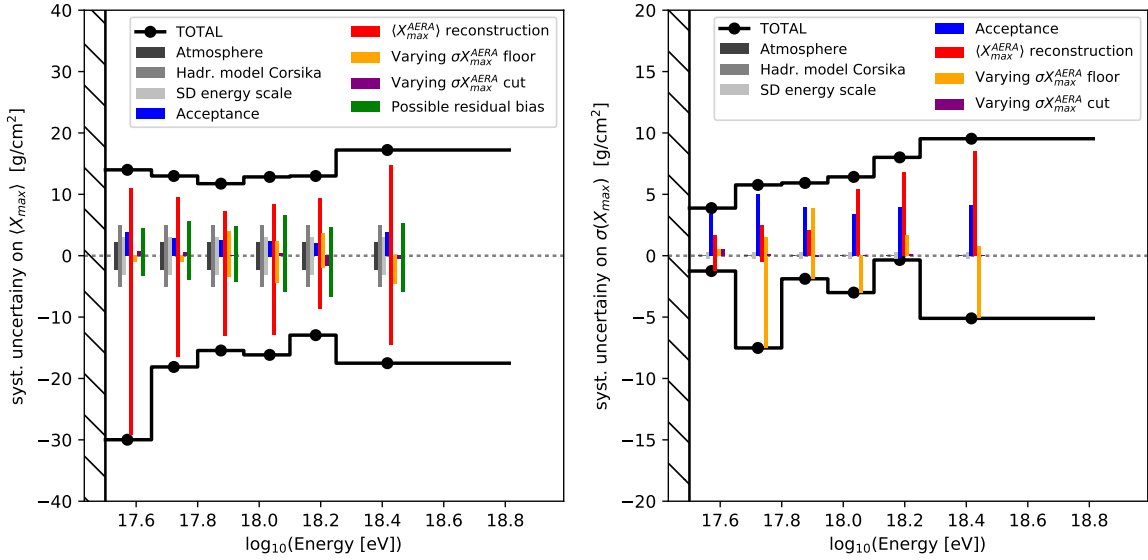## 6. Moments of the $X_{\max}$ Distribution

In Fig. 3 we show the two central moments of the $X_{\max}$ distribution from a bias-free set of 594 showers. For this, we have applied anti-bias cuts on the initial set of 2153 events. We require that at least 90% of the $X_{\max}$ values in a Gumbel distribution [14, 15] for a pure proton or pure iron nuclei composition, at the energy of the measured event, would have been reconstructed successfully (the remaining effects will be accounted for in systematic uncertainties in Sec. 7). This has been determined by evaluating if we would have successfully reconstructed the simulated showers that we have for a particular measured event. Furthermore, the trigger of the SD only becomes fully efficient above $E = 10^{17.5}$ eV, so we cut the showers at lower energy.

To interpret $X_{\max}$ in terms of mass composition, we compare the two central moments of the $X_{\max}$ distribution to the predictions of three hadronic interaction models for a pure proton and pure iron nuclei composition (red and blue lines in Fig. 3). We show that AERA sees a light to light-mixed composition in the energy range between $10^{17.5}$ and $10^{18.8}$ eV, the energy range where it is expected that the origin of cosmic-ray sources transitions from being Galactic to extra-galactic. Furthermore, we compare our results to the Auger FD results and see compatibility within uncertainties for both moments of $X_{\max}$.

7. Systematic Uncertainties on $X_{\max}$ and $\sigma(X_{\max})$

For the central moments of $X_{\max}$ in Fig. 3 we have also accounted for various systematic uncertainties (see Fig. 4). The primary uncertainty comes from the $X_{\max}$ reconstruction method itself (red bars). Using the reconstruction of our simulated showers we have calculated the effect on the central moments of $X_{\max}$. The effect depends on the composition itself. To be conservative we make no assumption on the composition and take the range of bias for a pure proton and bias for a pure iron nuclei composition as our systematic uncertainty. Further contributions arise from the acceptance cuts performed in the previous section. We quantify the effect of the lower detection efficiency of showers with the deepest $X_{\max}$ on the central moments of $X_{\max}$ by evaluating again the effect on our simulated showers for the case of a pure proton or pure iron nuclei composition. This results in a small contribution of a few $\mathrm{g\,cm^{-2}}$ (blue bars). We also account for two smaller contributions from the effects of low-number statistics in the calculation of $\langle X_{\max}\rangle$ and $\sigma(X_{\max})$. The first (orange bars) accounts for single data points with very low $X_{\max}$ uncertainties disproportionally contributing and skewing the final moments. The second (magenta bars) accounts for very large uncertainties affecting the calculation. All calculations are repeated with varying threshold values and the variation of the results is shown as systematic uncertainties.

Finally, we account for several small systematic uncertainties from our air shower simulations [9]. The energies of the air showers in these simulations, taken from the measured SD energies, rely on the energy scale used in SD and can shift the $X_{\max}$ scale, which depends on the energy, by $2.9\,\mathrm{g\,cm^{-2}}$ (and $0.3\,\mathrm{g\,cm^{-2}}$ for $\sigma X_{\max}$). Furthermore, the choice of the hadronic

Figure 4: (Left) Overview of upper and lower values of the systematic uncertainties on $\langle X_{\max} \rangle$, the mean of the $X_{\max}$ distribution. The individual contributions to the total uncertainty are plotted as bars centered in each of the energy bins. The total uncertainty (black lines) is the quadratic sum of the individual contributions. The weighted average of the energy in each energy bin is shown as black circles. The hatched region indicated the cut on energy imposed earlier. (Right) Overview of systematic uncertainties on $\sigma(X_{\max})$, the true spread of $X_{\max}$.

interaction model ($5\,\mathrm{g\,cm^{-2}}$) and the uncertainty in the GDAS atmospheric model ($2.2\,\mathrm{g\,cm^{-2}}$) also provide similar small effects on the first moment of $X_{\max}$.

As an additional check on our event selection bias, we have quantified any residual bias by investigating the mean $X_{\max}$ as a function of the zenith angle, azimuth angle, geomagnetic angle (angle between the shower direction and the geomagnetic field), and shower core position. We have found no significant trends as a function of these geometry-dependent parameters, but have quantified the allowed possible bias within the trend uncertainties as possible residual bias. The effect is around 3 to $10\,\mathrm{g\,cm^{-2}}$, increasing with energy, respectively (green bars in Fig. 4). The total systematic uncertainty is obtained by the quadratic sum of all individual contributions and is shown in Fig. 4 as the black lines, as a function of energy.

8. Conclusion

We have presented a method to reconstruct the depth of shower maximum of air showers using a sparse radio array by matching dedicated CORSIKA/CoREAS simulations to radio observations. We implemented steps to correct reconstruction biases inherent to this type of method and we have performed an extensive investigation of systematic uncertainties. Furthermore, we showed that we are able to obtain an $X_{\max}$ resolution of better than $15\,\mathrm{g\,cm^{-2}}$. With this we are able to show a (light)-mixed mass composition at energies between $10^{17.5}$ and $10^{18.8}$ eV, compatible with earlier fluorescence measurements at Auger. Additionally, we have compared the $X_{\max}$ reconstruction of a subset of showers measured simultaneously and independently with AERA and the FD and have shown there to be no significant bias between the two methods.

References

[1] P. Abreu *et al.* (Pierre Auger Collaboration), *J. Instrum.* **7** (2012) P10011

[2] M. De Domenico *et al.*, JCAP **07**, 050 (2013).

[3] S. Buitink et al., *Nature* **531** (2016) 70

[4] D. Heck et al., *FZKA Tech. Umw. Wis. B* **6019** (1998)

[5] T. Huege et al., *AIP Conf. Proc.* **1535** (2013) 128-132

[6] S. Ostapchenko, *Nucl. Phys. B-Proc. Sup.* **151** (2006) 143-146

[7] M. Bleicher, *J. Phys. G* **25** (1999) 1859–1896

[8] P. Mitra *et al.*, Astropart. Phys. **123**, 102470 (2020).

[9] B. Pont, Ph.D. thesis, Radboud University, 2021.

[10] C. W. Fabjan, F. Gianotti, Rev. Mod. Phys **75**, 1243 (2003).

[11] A. Yushkov [for the Pierre Auger Collaboration], PoS(ICRC2019)482

[12] J. Bellido [for the Pierre Auger Collaboration], PoS(ICRC2017)506

[13] A. Aab *et al.* (Pierre Auger Collaboration), Phys. Rev. Lett. **126**, 152002 (2021).

[14] S. Petrera, personal communication (October 30, 2020).

[15] M. de Domenico *et al.*, J. Cosmol. Astropart. P. **07**, 050 (2013).

PoS(ARENA2022)044